

General Disclaimer

One or more of the Following Statements may affect this Document

- This document has been reproduced from the best copy furnished by the organizational source. It is being released in the interest of making available as much information as possible.
- This document may contain data, which exceeds the sheet parameters. It was furnished in this condition by the organizational source and is the best copy available.
- This document may contain tone-on-tone or color graphs, charts and/or pictures, which have been reproduced in black and white.
- This document is paginated as submitted by the original source.
- Portions of this document are not fully legible due to the historical nature of some of the material. However, it is the best reproduction available from the original submission.

X-621-71-232
PREPRINT

NASA TM X- 65568

OBSERVED SOLAR GEOMAGNETIC CONTROL OF THE IONOSPHERE: IMPLICATIONS FOR REFERENCE IONOSPHERES

H. A. TAYLOR

JUNE 1971



GODDARD SPACE FLIGHT CENTER
GREENBELT, MARYLAND

FACILITY FORM 602

N71-27671

(ACCESSION NUMBER)

42

(THRU)

63

(PAGES)

TMX-65568

(CODE)

13

(NASA CR OR TMX OR AD NUMBER)

(CATEGORY)

X-621-71-232

OBSERVED SOLAR GEOMAGNETIC CONTROL OF THE IONOSPHERE:
IMPLICATIONS FOR REFERENCE IONOSPHERES

H. A. Taylor

June 1971

GODDARD SPACE FLIGHT CENTER
Greenbelt, Maryland

OBSERVED SOLAR GEOMAGNETIC CONTROL OF THE IONOSPHERE:
IMPLICATIONS FOR REFERENCE IONOSPHERES

H. A. Taylor

Goddard Space Flight Center
Greenbelt, Maryland

ABSTRACT

The recent availability of nearly continuous, pole to pole profiles of ionospheric composition permits the first detailed view of the significance of solar-geomagnetic processes in determining the distribution of ionospheric components. Bennett RF spectrometer results from the polar orbiting OGO 2, 4 and 6 satellites reveal dominant longitudinal variations superimposed upon the latitudinal distributions of each ion specie. The longitudinal variation is important throughout the altitude range of these satellites, being observed in the distributions of molecular ions (N_2^+ , NO^+ , O_2^+) in the range 400-700 km., and persistent also in the distributions of the light ions (H^+ , He^+) observed near apogee in the range 800-1100 km. The magnitude of the longitudinal variation may be quite pronounced, with the ambient concentration of O^+ observed at a given altitude and geodetic latitude varying by as much as an order of magnitude between two opposing longitudes, during relatively quiet magnetic conditions ($Kp \leq 2$). Although the character and magnitude of the longitudinal variations may be different for different ions, a broad and persistent pattern is observed in which the average longitudinal variation appears to be well

ordered in terms of solar-geomagnetic geometry. Because of the prominence of the longitudinal variation observed during just one earth rotation, the identification of seasonal, diurnal, and annual variations of the ion composition requires selective analysis of data having a high degree of spatial resolution. Such a study has been conducted with OGO-6 ion results, revealing that (1) seasonal variations in the ion distributions are generally repeatable, and (2) the annual variation in the topside O^+ and H^+ content and distribution between 1969-70 was minimal. These results would have been largely obscured in the absence of the longitudinal resolution required to provide data at appropriate solar-geomagnetic orientations. This study emphasizes the importance of magnetic field control in regulating the ion distributions, and suggests the need for the use of improved coordinate systems for the correlation of satellite observations and the development of ionospheric models.

1. Introduction

Beginning with the launch of OGO-4 in October, 1965, sets of nearly continuous, high resolution direct measurements of thermal ion composition have been obtained for a wide range of locations and geophysical conditions. Together, these results comprise the most complete empirical evidence for the complexity of the distributions of the principle ions which populate the ionosphere within the altitude range of approximately 400-1100 km. An outstanding feature of these results has been the identification of a broad and persistent longitudinal variation observed in the pole to pole profiles of ion composition obtained as the earth rotates beneath the relatively fixed satellite orbit. The pattern of the longitudinal variation has been associated with the wobble of the geomagnetic field relative to the earth-sun orientation, and has been identified in earlier studies as evidence for a "solar-geomagnetic" seasonal variation [1]. Preliminary studies of OGO-4 results have shown that the longitudinal variation is extremely important for global studies of the O^+-H^+ transition level, as well as investigation of the global prominence of ionized helium [2].

Although a number of previous investigators have found some evidence of the longitudinal variation, a definitive identification of this phenomena has awaited the availability of measurements from the OGO satellites which permit nearly continuous sampling of the longitudinal variation, as the earth rotates beneath

the relatively fixed position of the satellite orbit. The fact that ion composition is recorded for complete orbits, on a continuing basis, is a major factor in the identification of the ionospheric features described in this paper.

In this study, we examine the longitudinal variation more extensively, using data sets obtained from the OGO-6 ion spectrometer during the period 1969-70. During this interval, the experiment was operated continuously, and the resultant data is interrupted only occasionally by gaps attributable to spacecraft operations and data tape processing. Accordingly, for most data sets to be studied, longitudinal profiles of the distributions of each of the ion constituents are obtained on a nearly continuous basis, with a separation of approximately 25° of longitude between consecutive orbits, with a period of approximately 105 minutes. In the long sweep mode, the sampling resolution, determined by the spectrometer sweep rate of approximately 35 seconds is about 3° of latitude between consecutive samples of a given ion along the orbital path. Significant longitudinal variations have also been discovered in data obtained in the short sweep mode which provides a resolution of 0.2° latitude between samples [3].

Although the orbital inclination is nearly polar (82°) the tilt of the dipole axis results in a variable range of latitude coverage between orbits. Wherever possible in the results which follow, an attempt is made to identify the longitudinal variation under the most comparable conditions of altitude and latitude, so

as to rule out possible confusion produced by changes in these variables. This objective, combined with the precession of apogee-perigee versus latitude, season, and local time significantly limits the number of data sets appropriate for the identification of fundamental variations. Within these limits, the results have been chosen to be representative of the diurnal, seasonal, and annual variations observed independently, at particular times and locations.

2. Results

2.1 Ion Distributions in Geodetic Latitude

The longitudinal variation has been observed throughout the ion composition, extending from the body of molecular ions populating the lower thermosphere to the light ions of the plasmasphere. To establish the significance of the geomagnetic field in regulating the distributions of these ions, we first examine the longitudinal variability of several of the more prominent ions, as a function of geodetic latitude.

In Figure 1a, profiles of O_2^+ observed near 0630 LT, at $50^\circ E$ and $154^\circ W$ long., respectively, illustrate the extent of the longitudinal variation observed at lower altitudes. As an example, it may be seen that the ambient concentrations of O_2^+ at the equator, near 400 km., differ by as much as a factor of 4 between these contrasting longitudes. At low-southern latitudes, the difference increases to a factor typically near 6, although the zenith angle variation with latitude remains unchanged between these two passes. Note also that the altitude variations between

the two passes are relatively minor at low latitudes, where significant concentration differences are observed. The magnetic conditions preceding each of these passes were also similar. Defining the maximum value of Kp in the 12-hour interval preceeding the pass as Kp₋₁₂, Kp₋₁₂ = 3- for the March 15 pass and Kp₋₁₂ = 2+ for the March 17 pass. Accordingly, it is clear that the changes with longitude observed in the O₂⁺ distributions, including both the significant change in total concentration, as well as the distinct shift in the N-S symmetry of the distributions are indeed most prominent and are not readily explained when viewed in the geodetic coordinate system.

In Figure 1b, we examine the distributions of O⁺ during northern summer, and near 1600 LT. Although at this time apogee occurs near the south pole, and significant altitude variations exist between the northern and southern hemispheres, the altitude versus latitude relationship for the two passes compared is very similar and, to a first approximation, altitude effects may be ruled out in considering the longitudinal variation. It may be seen that while the shape and amplitude of the O⁺ distributions are similar in the northern summer hemisphere, a distinct variation begins to occur below about 30° in the southern winter hemisphere. At 60°S, a difference of an order of magnitude is observed between the O⁺ concentrations, although altitude, zenith angle, and prior magnetic activity are closely comparable.

In Figure 1c, the longitudinal variation in He^+ is shown for equinox, near 0500 LT. In this case, with apogee near the equator, the altitude-latitude relationship is identical for the 2 passes, and significant differences are observed in the He^+ distributions at the contrasting longitudes. In particular, a pronounced equatorial trough is observed in He^+ on the pass near 160°W long., where the He^+ distribution drops by about an order of magnitude near the equator, relative to the mid latitude concentration levels, near $\pm 30^\circ$. Note that the trough is broader, although much less pronounced, at the 100°E position. Once again, these data have been chosen for comparable periods of relatively quiet magnetic activity.

In Figure 1d, contrasting distributions of H^+ obtained during northern summer and near midnight local time exhibits significant differences between longitudes. Both the depth and position of the high latitude proton trough are seen to change significantly with longitude. (Although some difference in the H^+ distributions might be expected as a result of the unavoidable difference in Kp history, this would not be in the direction of reducing the observed longitudinal variation, since the plasmasphere is observed to shrink with increasing Kp.) Like the O^+ distributions of Figure 1b, the H^+ distributions of Figure 1d exhibit similarity in the summer hemisphere, and yet show prominent differences in the southern winter hemisphere. Like O^+ , the H^+ distribution appears to be 'tilted' toward the winter hemisphere, where a winter time ion

depletion appears to be emphasized at certain longitudes.

From the foregoing ion distributions, as well as from the distributions of other ions observed at a variety of local times and seasons, it is clear that pronounced and persistent variations in both the concentration and distribution of ionization is encountered with changing longitude. The persistence of the observed variations strongly suggests that the geomagnetic field must play a dominant role in regulating the ion distribution. For this reason, we next examine the longitudinal variation in terms of dipole latitude. For each of the time periods identified in Figures 1a-d, we have selected sets of ion distributions representative of the longitudinal variation encountered throughout a complete earth revolution. In Figures 2a-d, isometric displays of ion distribution sets are given for each of the local times associated with the profiles of Figures 1a-d, respectively.

In Figure 2a, it may seem that the latitudinal distributions of O_2^+ change noticeably as the earth rotates beneath the relatively fixed orbit during the two day interval of March 15-17. In this figure, the O_2^+ profiles are arranged to illustrate a distribution pattern which appears to be correlated with the changing solar-geomagnetic geometry, indicated by the angle α , which is defined in the noon local time plane as the angle between the earth-sun line and the dipole equator. For the March condition of equinox, the amplitude of α oscillates between $\pm 11^\circ$ (the displacement of the magnetic axis) during the course of one earth rotation.

Similarly, the latitudinal distributions of O_2^+ exhibit a cyclic variation, with a tendency for broader and more symmetric distributions at eastern longitudes ($-\alpha$) relative to the western longitudes ($+\alpha$). In addition to this broad pattern, the O_2^+ distributions also exhibit complex features at higher latitudes, beyond about $\pm 45^\circ$.

Further evidence for the link between the persistent longitudinal variation and the changing solar-geomagnetic orientation is given in Figure 2b. In this case, the O^+ distributions obtained near 1600 LT during the 3 day interval June 27-June 29, reveal a very pronounced correlation between the longitudinal variation in O^+ and the angle α . Because the sun is near the summer solstice position in June, the angle α remains positive throughout the earth rotation, and reaches its maximum amplitude near $7^\circ W$ long. The variation in the O^+ distributions follows a similar pattern, with the southern (winter) hemisphere concentrations falling off dramatically in the range where α is maximum. In the northern (summer) hemisphere, the amplitude and shape of the O^+ distributions is relatively constant. From this pattern, it is seen that for solar-geomagnetic winter conditions, the apparent seasonal variation in O^+ is most pronounced, with "maximum winter" (highest α) being lower by as much as an order of magnitude than concentrations observed at "minimum winter" (minimum α). Again, it should be noted that while the altitude versus dipole latitude relationship is of course not identical for each ion profile, a direct comparison

of pass to pass variations indicates that the range of altitude variability is much less than might be required to explain the observed longitudinal variation in concentrations.

As indicated previously, the longitudinal variation persists in the light ions as well, and in Figure 2c we see an example of the variability in He^+ observed near 0500 LT during September 22-23. A significant feature of the longitudinal pattern in He^+ is the changing prominence of the equatorial trough, which is observed to be narrow and deep for the $+\alpha$ condition, in contrast to being broad and relatively shallow for longitudes for which α becomes negative. In addition, although the effect is somewhat more subtle, there is a tendency for He^+ to persist to higher latitudes at magnetic winter (negative α) locations, which is consistent with earlier evidence of a winter bulge in He^+ [2].

The final example of the pattern of longitudinal variability is given in Figure 2d, in which the distributions of H^+ near 2400 LT are shown for the period July 24-30. In this case the southern winter hemisphere distributions of H^+ exhibit a pronounced variation with longitude. At the positions of extreme solar-geomagnetic winter (maximum α) the high latitude trough in H^+ becomes much deeper and moves to its highest latitude position. Although it cannot be readily shown in the same figure, the northern summer distributions of H^+ exhibit a comparatively insignificant variation with longitude. As in the case of O^+ shown in Figure 2b, the longitudinal variation in H^+ is emphasized in the winter hemisphere. It

is emphasized that, for this data set, the longitudinal variation is observed following periods of relatively quiet magnetic activity, with $Kp_{-12} \leq 3$ for all profiles in the set.

2.2 Identification of Basic Ionospheric Features

Having identified the importance of the longitudinal variation and the qualitative usefulness of the parameter α , it becomes evident that the identification of ionospheric features such as the diurnal or local time variation is directly dependent upon the ability to obtain data under comparable solar-geomagnetic orientations. In the following examples we attempt to identify the repeatability and predictability of certain basic ionospheric features, using the parameter α as a selection guide.

2.3 The Persistence of Winter-Summer Characteristics of H^+ and O^+ Near Dusk

The significance of the longitudinal variation as a parameter for guiding the identification and selection of comparison data is illustrated in Figures 3 and 4, which show the persistence of winter-summer characteristics in H^+ and O^+ , respectively, as observed in both the northern and southern winter hemispheres, near dusk local time. Because of the nature of the OGO-6 orbit, this comparison between data obtained in June and December, 1969, results in a local time separation of approximately 2 hours (1600-1800 LT), which adds some evidence of the stability of the ion distributions with respect to local time. In Figure 3, the profile H^+ obtained during northern winter (December) shows remarkable agreement with the profile obtained during southern winter (June). Note that the

longitudes are deliberately chosen to be different, in order to obtain equal and opposite values for α . As before, these passes have been chosen to provide essentially identical altitude versus latitude relationships as well as similar magnetic activity histories.

In Figure 4, O^+ profiles obtained simultaneously with the H^+ profiles of Figure 3 indicate a similar persistence of the seasonal variation in O^+ , between hemispheres. The high latitude, winter hemisphere portions of both the O^+ and H^+ distributions exhibit complex recovery regions which are believed to be associated with auroral zone disturbances. The irregularity of this region confuses the seasonal pattern somewhat, although the general features are fully recognizable. It is emphasized, that for both O^+ and H^+ , the seasonal persistence which is illustrated is found only by comparing profiles observed under comparable solar-geomagnetic orientations. It is most significant, that if the comparisons had been performed at the same longitude for both seasons, the close agreement in the ion distributions would have been lost. As selected, however, these profiles reflect nearly identical solar-geomagnetic seasonal conditions and accordingly show good agreement.

2.4 Diurnal Variations in H^+ and O^+

Recognizing the significance of seasonal variations such as identified in Figures 3 and 4, we have attempted to identify an example of the day-night variation in the ion distributions for

equinox conditions. Unfortunately, data sets for equinox and with altitude symmetry about the dipole equator are limited to the dawn-dusk local time sector. Nevertheless, although we cannot yet identify the pure noon-midnight case, it is apparent from the examination of comparison data that the dawn profiles are indeed characteristic of the nighttime case, while the dusk profiles are rather typical of the daytime distributions. Accordingly, in Figures 5 and 6 we examine the contrast in dawn-dusk distributions of H^+ and O^+ , respectively.

In Figure 5, profiles of H^+ obtained at dawn (0500 LT) and dusk (1800 LT) provide evidence of a pronounced diurnal variation. At dusk, the mid-latitude concentrations of H^+ are considerably lower than at dawn, with differences as great as an order of magnitude near $\pm 45^\circ$. Consistent with this pattern, the light ion trough is much more pronounced at night with H^+ decreasing by as much as an order of magnitude within 10° of latitude.

As shown in Figure 6, the diurnal variation in O^+ is observed to be considerably more pronounced than the variation in H^+ . In particular, the extensive depletion of O^+ at low and mid latitudes at night is the dominant feature, with the concentrations of O^+ lower by a factor of more than two orders of magnitude near the equator at night. By comparing Figures 5 and 6, it is seen that during the day where O^+ is the dominant topside ion, the latitudinal decrease in H^+ toward the poles is relatively gradual, and for quiet, equinox conditions, the light ion trough is not sharply

defined. At night, however, where H^+ is the dominant topside ion, a much more steep and identifiable trough is formed in the proton distributions. Once again, it is emphasized that a selection on α has been used to identify the representative equinox condition. If data were to be selected at the same longitude for both dawn and dusk, the symmetry, and thus the comparability, in the distributions would be significantly degraded.

Several additional features of the day-night ion distributions of Figures 5 and 6 should also be noted. First, these profiles, in general, exhibit considerable symmetry in the N-S hemispheric distributions, consistent with the fact that these profiles reflect solar-geomagnetic equinox. The lack of seasonal asymmetry is particularly evident in the daytime distributions, which exhibit peaks in the distributions of both O^+ and H^+ at the dipole equator, as well as nearly identical concentrations of the respective ions between the northern and southern hemispheres. The nighttime distribution of H^+ also exhibits considerable N-S symmetry during equinox, although the symmetry of the companion O^+ distribution shown in Figure 6, is somewhat offset at low latitudes by a somewhat asymmetric hump, or equatorial increase. This unexpected increase in O^+ has been observed in other sets of nighttime data and is believed to be a characteristic feature, which will be the subject of a separate study.

2.5 Annual Variations in Topside Composition

In order to search for possible long-term variations in the content and distribution of the topside ionosphere, we have selected samples of O^+ and H^+ obtained at times separated by about 1 year. Consistent with the foregoing results, the local time regions selected for this comparison have been deliberately chosen so as to examine the behavior of both O^+ and H^+ under conditions for which each of these ions respectively becomes the dominant ion. Accordingly, in the results that follow we examine the behavior of O^+ on the dayside, and with perigee centered about the dipole equator. Conversely, for checking the long-term stability in H^+ , we will examine nighttime distributions obtained with apogee centered about the dipole equator. In order to obtain these conditions, it was necessary to select data obtained during July 1969 and 1970, for northern summertime conditions.

In Figure 7, we see essentially a lack of annual variation in the distribution of O^+ . Both the maximum concentration observed near the dipole equator, as well as the northern and southern hemisphere distributions of O^+ are quite comparable from one year to the next. Although some altitude variation between the two passes being compared was unavoidable, there appears to be no systematic relationship between the altitude differences and the relatively minor concentration differences observed at various latitudes. As noted in Solar Geophysical Data [4] the periods of July 1969 and 1970 are characterized by similar solar activity levels,

representative of conditions near the maximum of solar cycle 20, and thus no significant difference in the O^+ content would be expected. It is emphasized that, in order to identify the similarity in the O^+ distributions observed one year apart, it was necessary to select passes having nearly identical α orientations. In this case the α values are 8° and 11° respectively, corresponding to near minimum solar-geomagnetic seasonal conditions, even though the month of June is characteristic of geodetic northern summer. The N-S symmetry reflected in the O^+ profile is consistent with the relatively low values of α , reflecting near solar geomagnetic equinox, rather than northern summer.

In Figure 8 we observe a similar long-term repeatability in the distributions of H^+ observed between July 1969-70, but for higher values of α . Accordingly, in addition to the evidence of a lack of any pronounced annual variation in H^+ at night, there is also superimposed the consistent evidence of a slight asymmetry in the N-S distributions, with the southern or wintertime distributions being somewhat lower in concentration for a given dipole latitude. As a result of orbit phasing, comparison of data separated by 1 year also requires a separation of 3 hrs. LT, for apogee/perigee centered above the dipole equator. Again this LT separation adds some evidence of the range of repeatability of the ionosphere. With regard to the relatively small altitude and Kp differences involved in the comparison, there is no evidence that changes in either of these parameters significantly influence the

overall comparison. In view of these qualitative remarks, we conclude that the repeatability in the O^+ and H^+ distributions over a period of one year is indeed pronounced, and that within several hours variation near midnight and noon, respectively, the ionosphere may be reasonably predictable, near solar maximum.

3. Discussion

3.1 Evidence of Solar-Geomagnetic Control

Overall, the foregoing results contribute evidence for a more pronounced solar-geomagnetic control of topside ionization than has been generally recognized heretofore. Although earlier satellite studies [5] [6] [7] [8] provided important clues relative to the significance of the geomagnetic control of ionization, the recognition and documentation of the global longitudinal variation which appears to persist throughout the ion composition has awaited the nearly continuous data coverage made possible by the OGO satellites. As the results indicate, we now see that the longitudinal variation in the latitudinal distributions of a given ion may vary remarkably between two different geographic and or geomagnetic locations during the course of a given moderately quiet day. Accordingly, it has become increasingly clear that correlative studies as well as the identification of certain boundary values for charged particle models must take into account the significance of the longitudinal variation. As implied by the present results, studies of seasonal variations, examination of storm-time variations, and other studies involving a close

comparison of spaced observations from satellites will require selection for comparability of solar-geomagnetic coordinates.

The observed dominance of the geomagnetic field in ordering the ion distributions points toward still further complications in the process of selecting satellite observations for correlative and model studies. Since it is clear that the ions are constrained to move along the magnetic field lines, there are several physical processes which may be tentatively suggested as possible mechanisms contributing to the observed patterns of longitudinal variation in the ion distributions.

The first such mechanism is the action of the neutral thermospheric wind in inducing large-scale plasma transport by means of coupled ion drag, directed along magnetic field lines. As shown by the work of Kohl and King [9] the magnitude and direction of thermospheric winds are sufficient to produce F region anomalies observed within the ionosphere. The likelihood that winds may contribute to longitudinal shifts in the O^+/H^+ transition level has been demonstrated empirically using ion composition data from Explorer-32 [8].

As shown schematically in Figure 9, the component of the neutral wind acting along magnetic field lines will undergo distinct changes, as the magnetic field rotates relative to the fixed position of the neutral atmosphere pressure bulge. An added mechanism suggested in Figure 9 is the action of the polar wind [10] indicated by the outgoing arrows at high latitudes. The possible interaction of the upflowing polar

wind with the downflowing component of the thermospheric wind constitutes another example of a dynamic process regulated in part by the wobble of the geomagnetic field in the earth sun geometry.

Another possibility for explaining certain of the observed longitudinal variations may lie in the fact that the orientation between the satellite orbit and the geomagnetic field lines varies constantly as the earth rotates. If we assume that the ions are closely constrained to move along magnetic field lines, and that the ionization observed along the orbit results from the upward diffusion of ionization produced at some lower altitude along a given L shell, we may predict the possibility of what may be referred to as an "effective local time" variation in the ion distributions. As shown schematically in Figure 10, the locus in local time of the feet of the field lines intersecting the OGO-6 orbit may be distinctly different, between two widely spaced longitudes. Thus, depending upon the degree of control exercised by the field and upon the importance of diffusion processes in supplying the ionization observed in satellite altitude, the magnetically varying "effective local time" may possibly account for certain observations which appear as 'exaggerated' local time and seasonal variations. The investigation of the possible "effective local time" mechanism is currently under study and will be reported separately.

3.2 Evidence of Predictability in Ionospheric Distributions

Recognition of the solar-geomagnetic ordering of the ion distribution provides the tentative result that under certain conditions the topside ion composition may be reasonably predictable, with preliminary evidence that both wintertime and summertime distributions are maintained at the opposite poles, and that annual variations (near solar maximum) are not pronounced. In view of the dominance of the longitudinal variation, and of the relatively small amount of definitive data which may be obtained from a given satellite (due to orbital phasing etc.), however, it is recognized that the present evidence for repeatability and predictability is preliminary. Nevertheless, the observed day-night variation in O^+ and H^+ , as well as the evidence that the distributions of these ions may remain relatively unchanged over ranges of local time of at least 3 hours, is generally consistent with existing theory, and in good agreement with the ion composition results of Explorer 32 [11].

In summary, to be more conclusive in describing diurnal, seasonal, and temporal variations of the topside ion composition, a more thorough evaluation of the combined effects of changing solar-geomagnetic geometry and varying orbital position must be made. Selective analysis of more 'pure' data sets, free of magnetic storm activity, and descriptive of primary seasonal and local time orientations, and with altitude effects removed, is a prerequisite for developing a clearer empirical model of the ion composition.

References

- [1] H. A. Taylor, Jr., Planetary and Space Science, 19, 77, (1971).
- [2] H. A. Taylor, Jr., et al., Space Research X, (1970).
- [3] H. A. Taylor, Jr., et al., NASA/Goddard Report No. X-621-71-227 (1971).
- [4] Environmental Research Laboratories Solar Geophysical Data Descriptive Text, (1971).
- [5] P. J. Bowen, et al., Proceedings of the Royal Society, 281, 504, (1964).
- [6] W. C. Knudsen, Journal of Geophysical Research, 72, 1941, (1967).
- [7] S. Chandra, et al., Journal of Atmospheric and Terrestrial Physics, 29, 259, (1967).
- [8] H. C. Brinton, et al., Space Research X, (1970).
- [9] H. Kohl, et al., Journal of Atmospheric and Terrestrial Physics, 29, 1045, (1967).
- [10] P. M. Banks, et al., Journal of Geophysical Research, 73, 6846, (1968).
- [11] H. C. Brinton, et al., Journal of Geophysical Research, 74, 4064, (1969).

Figure 1a-d. Examples of pronounced variation in ion distributions observed at positions of contrasting longitude. The notation $K_p -12$ refers to the maximum value of the planetary magnetic index K_p recorded during the twelve hour interval preceding the UT corresponding to the ion profile. The local time specified at the geodetic equator is measured as the orbit crosses the equator. The single time specified in each plot is chosen as representative of the time interval covered by the passes being compared. In panel b, the altitude distribution for the two passes is sufficiently identical that the data appears in the form of a single curve.

Figure 2a-d. Isometric displays of sets of ion profiles obtained during time intervals corresponding to the profiles shown in Figure 1 a-d. The profiles are plotted as functions of geodetic longitude, dipole latitude, and ion concentration. The angle α , measured at local noon, is defined at any longitude as the angle between the earth sun line and the dipole equator. The altitude profile indicated on the right hand plot in each family is representative of the altitude-latitude relationship characteristic of the family. The local time specified also represents a typical value for the series of satellite passes.

Figure 3. Evidence for the repeatability of summer-winter distributions of H^+ observed between June and December, 1969. The profiles are plotted without regard for polarity of latitude, with the summertime distributions on the left and winter distributions on the right, for both months. Note that the passes have been

selected so as to provide equal and opposite values of α , in order to obtain identical winter and summer solar-geomagnetic orientations.

Figure 4. Evidence of the summer-winter repeatability in the distributions of O^+ observed between June and December 1969. Above about 60° in the winter hemisphere, the distributions appear to reflect auroral irregularities, and thus are not expected to exhibit the same degree of seasonal repeatability as is evidenced at other latitudes.

Figure 5. A comparison of H^+ profiles obtained near dawn and dusk local time, respectively, and for near equinox conditions. The 0500 LT profile is representative of nighttime distributions, while the 1800 LT profile is more typical of dayside distributions. Note that the passes have been selected to provide identical α or solar-geomagnetic seasonal orientations. Also, α has been deliberately chosen to be of low amplitude, to be consistent with equinox conditions.

Figure 6. Day night variations in the distribution of O^+ observed simultaneously with the H^+ profiles of Figure 5.

Figure 7. Evidence for the lack of annual variation in the distribution of O^+ observed during local afternoon, between July 1969 and 1970. Profiles have been selected to obtain nearly identical values for α . Due to orbital phasing, a variation of 3 hours LT is unavoidable in the one year comparison.

Figure 8. Evidence of the repeatability in the distributions of H^+ observed following midnight between the periods July 1969 and 1970.

The passes have been selected to provide identical α orientations. Figure 9. A schematic representation of the variation of the neutral thermospheric wind (heavy arrows) with respect to the geomagnetic field lines, and the polar wind (small arrows). On the left, the neutral wind field is symmetric with respect to the dipole equator, and thus ion drag motion is equivalent in both the northern and southern hemispheres. On the right, for large values of α , the neutral wind field is distinctly asymmetric with respect to the geomagnetic field, resulting in a stronger wind component along closed field lines in the southern hemisphere relative to the northern hemisphere.

Figure 10. A schematic representation of the effective local time concept. The earth is viewed from the dusk meridian, with the left panel representing a longitude for which the magnetic field lines are tilted from the dayside in the north to the nightside in the south, while the right-hand panel represents the opposite case. The arrows represent the diffusion of ionization from a reference level (say 100 km) up to the altitude of the orbit. The dashed line represents the locus in local time of the feet of the field lines intercepted by the orbit. Thus, the "effective local time" of the source level ionization may change considerably between positions of contrasting longitude.

OGO-6 **A** MAR 15 '70 0300-0344UT 50°E K_p -12=3-
B MAR 17 '70 1612-1659UT 154°W K_p -12=2+

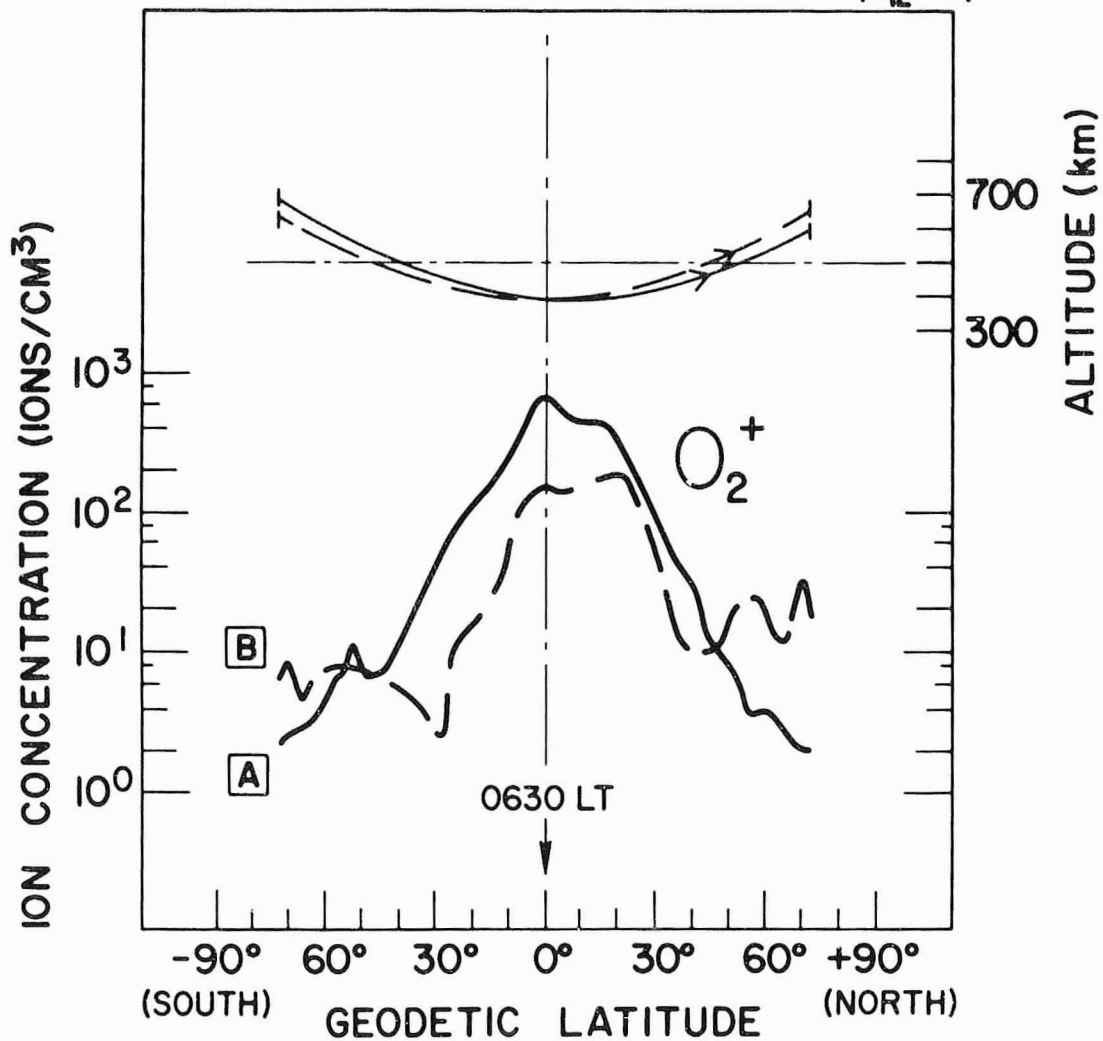


Figure 1A

OGO-6 **A** JUN 28 '69 0328-0413UT 175°W $Kp_{-12}=2_0$
 B JUN 29 '69 1600-1650UT 07°W $Kp_{-12}=1_0$

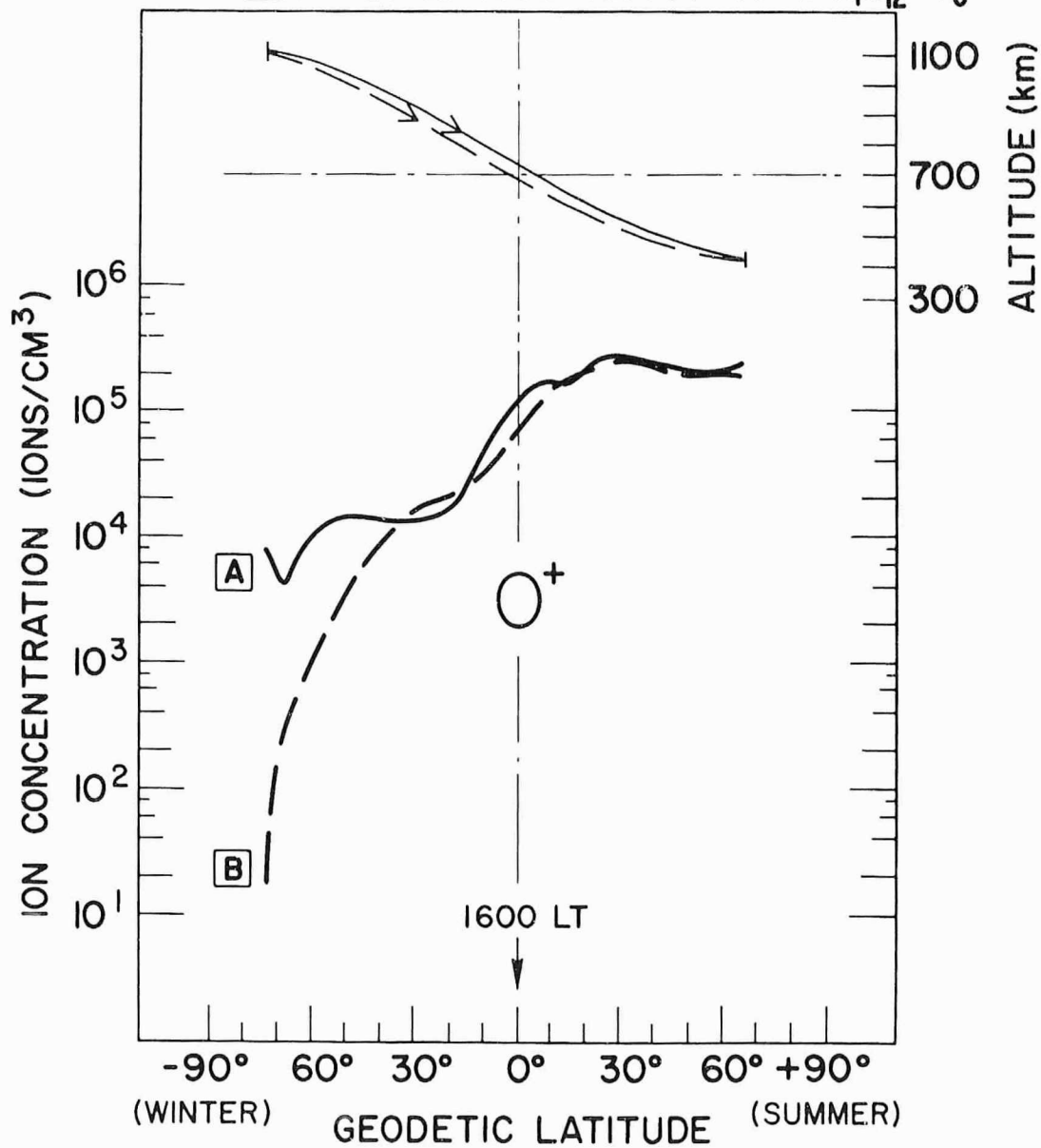


Figure 1B

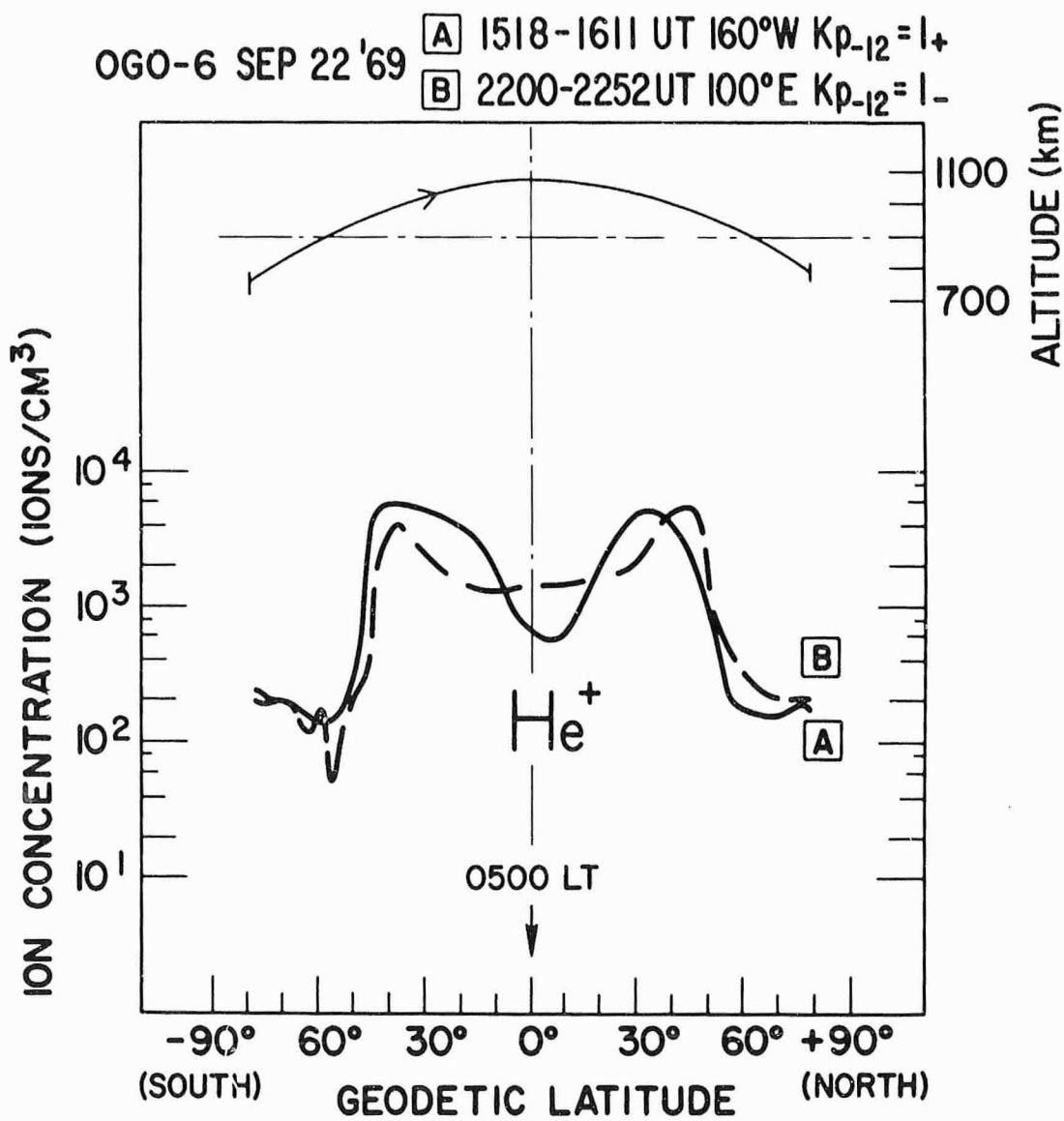


Figure 1C

OGO-6 [A] JUL 24 '69 0320-0409UT 42°W Kp₋₁₂=3-
 [B] JUL 29 '69 1746-1839UT 87°E Kp₋₁₂=0+

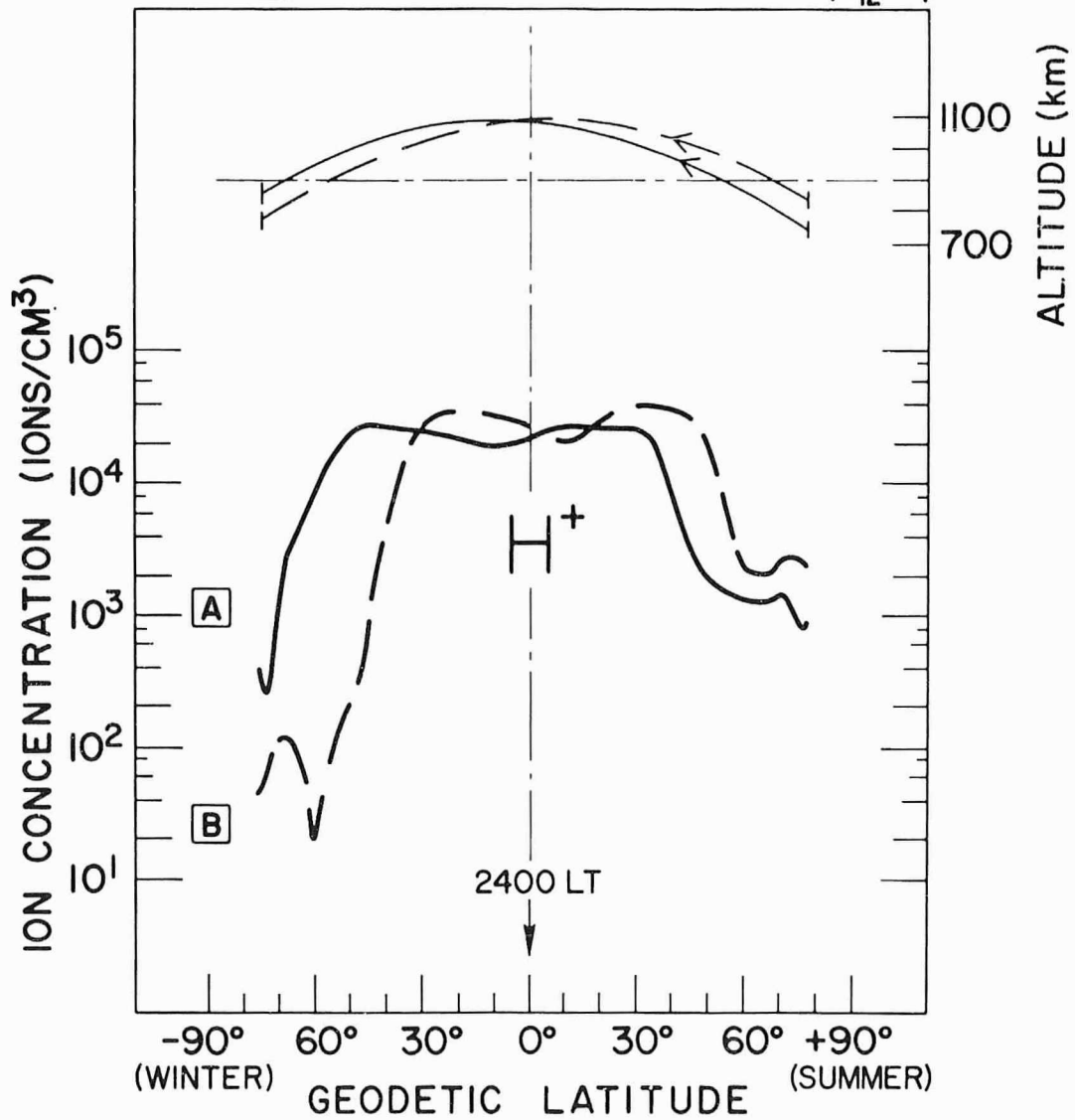
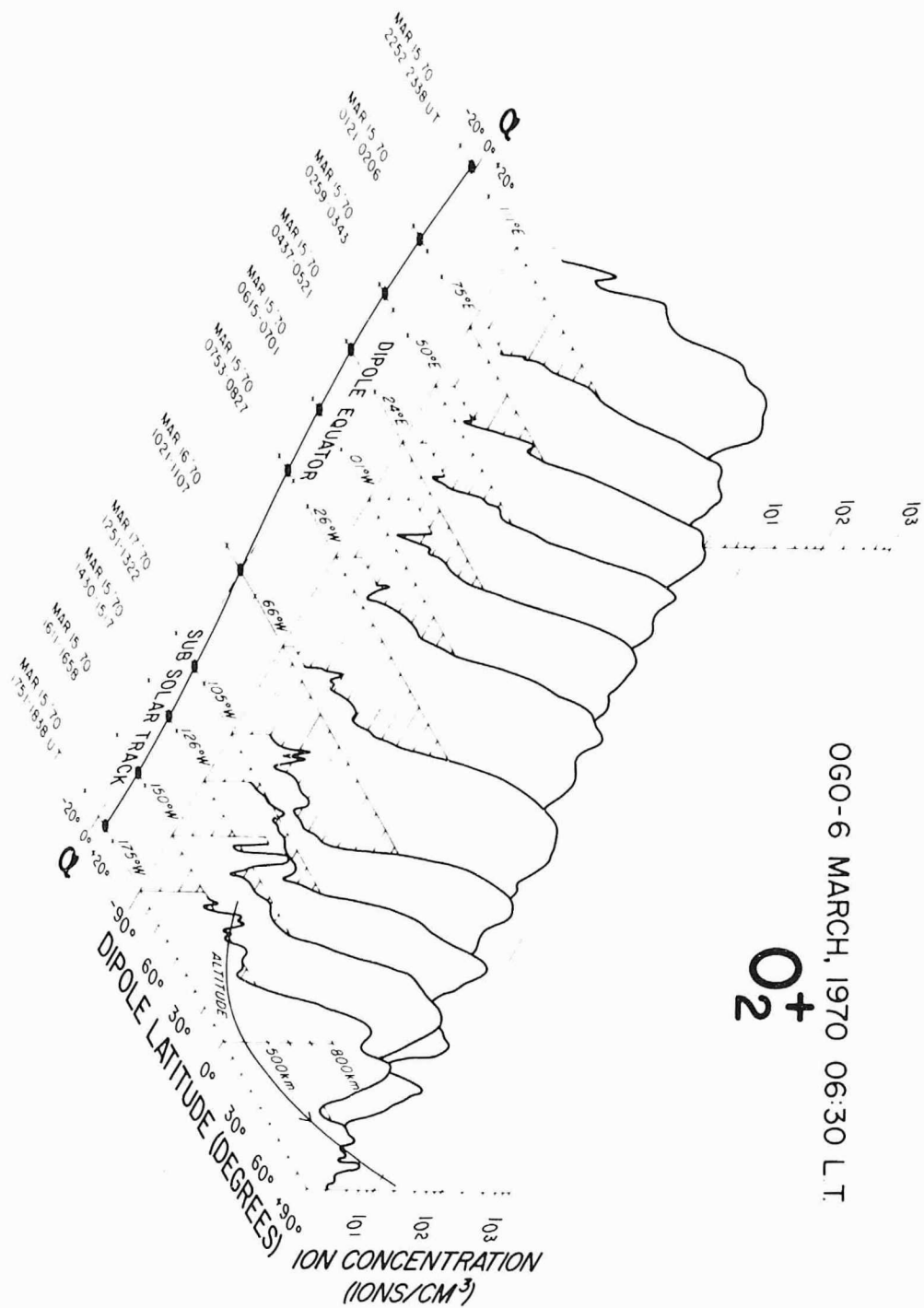


Figure 1D



OGO-6 MARCH, 1970 06:30 L.T.

O₂⁺

Figure 2A

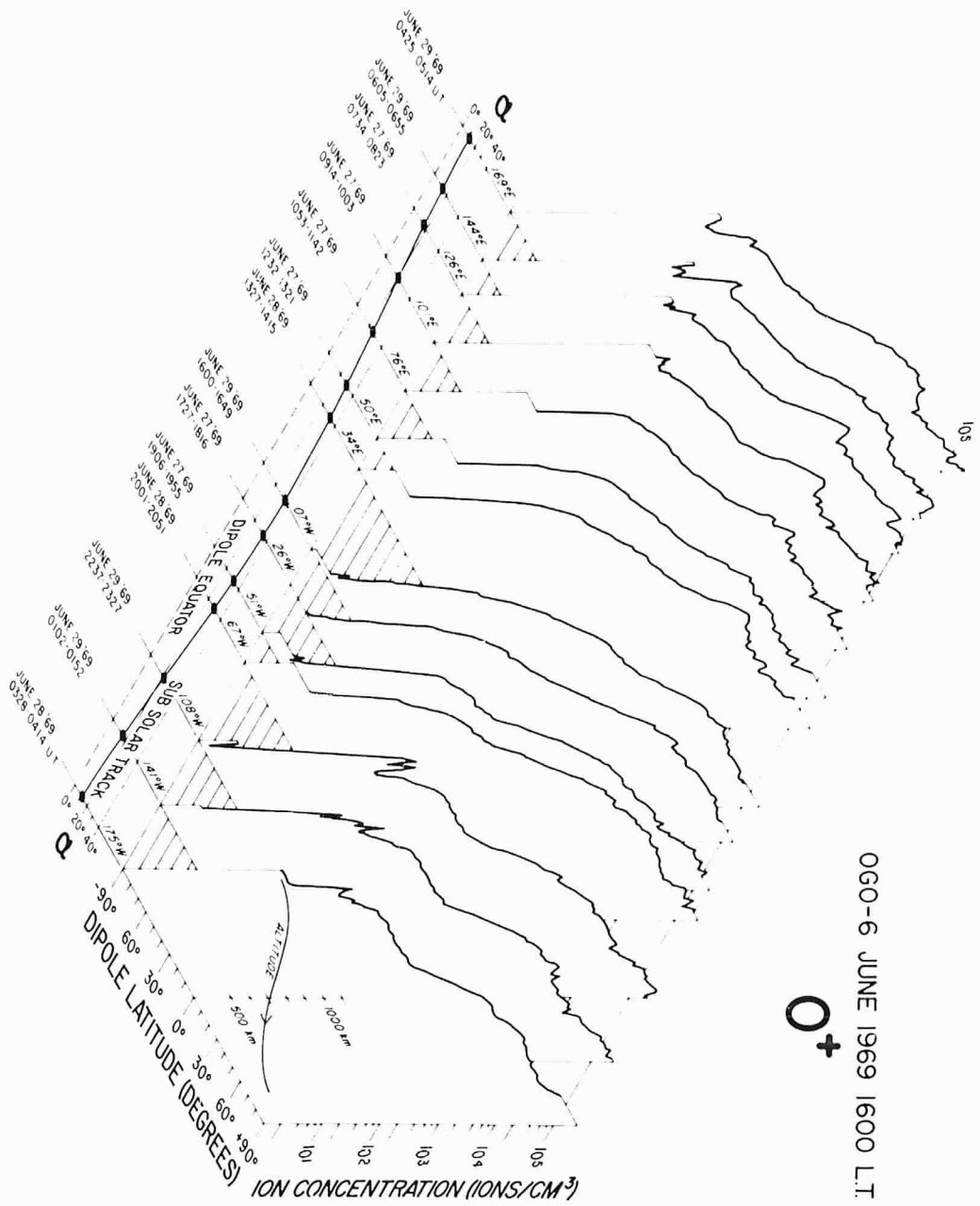


Figure 2B

060-6 SEPTEMBER, 1969

H^+

0500 L.T.

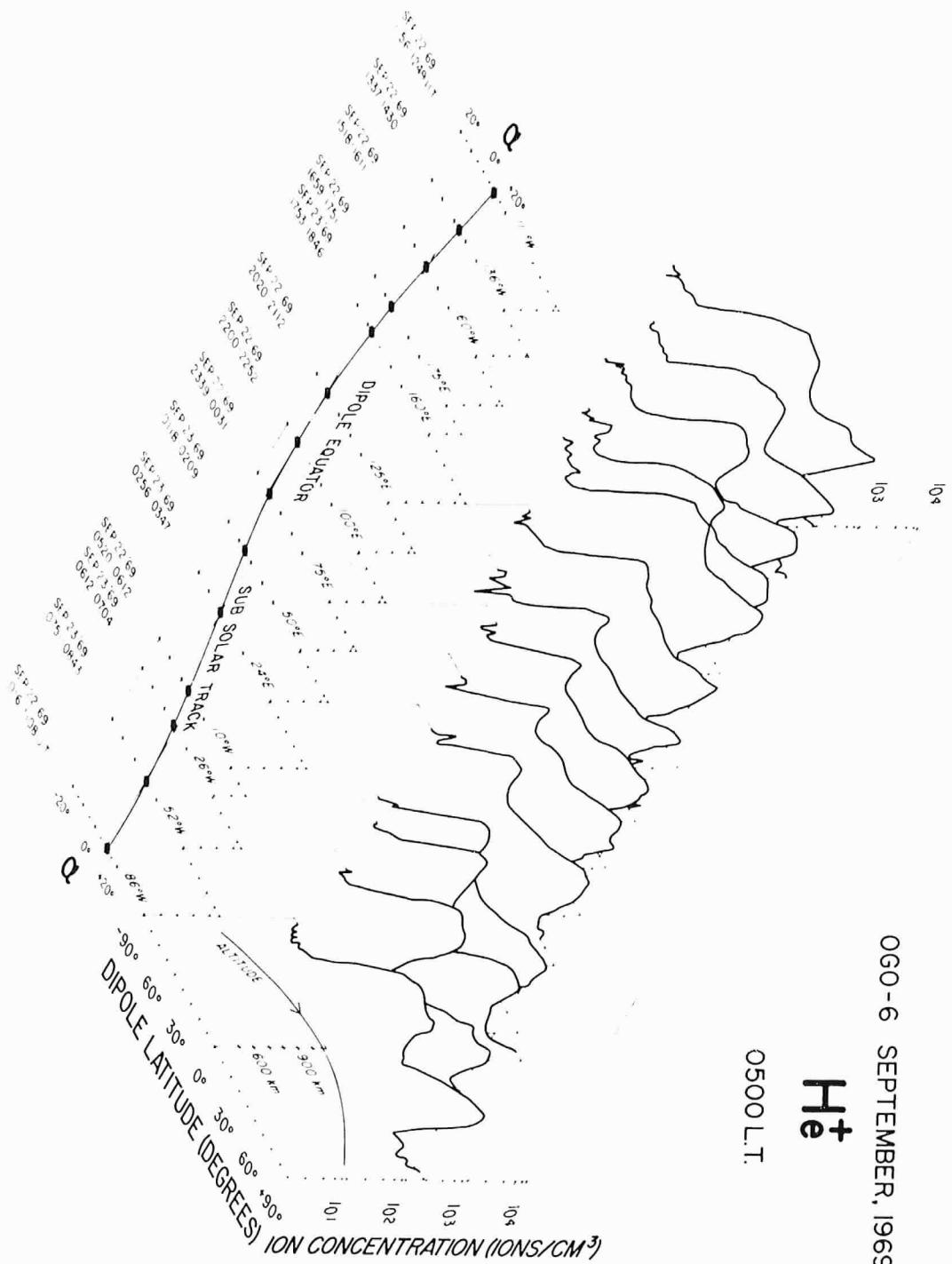


Figure 2C

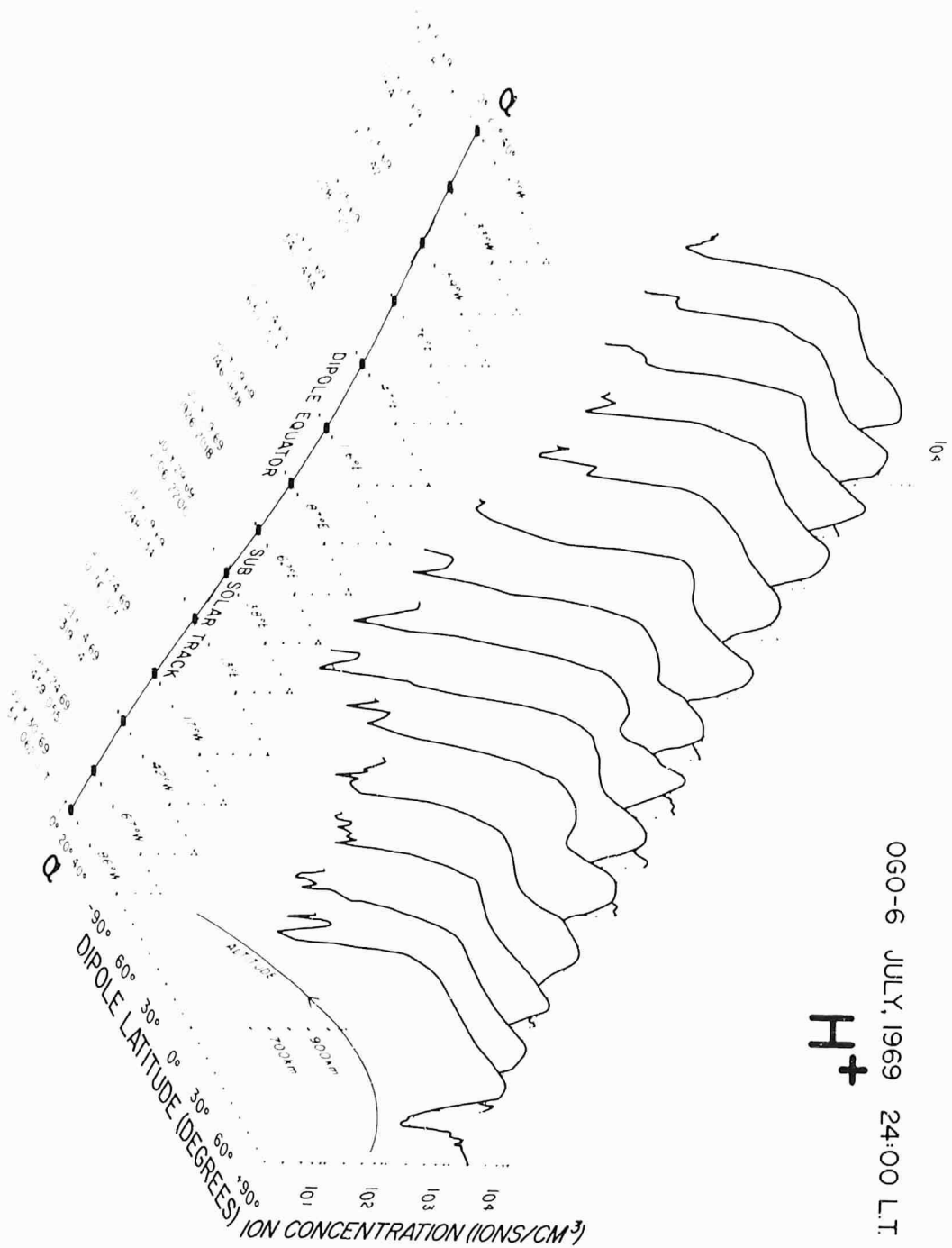


Figure 2D

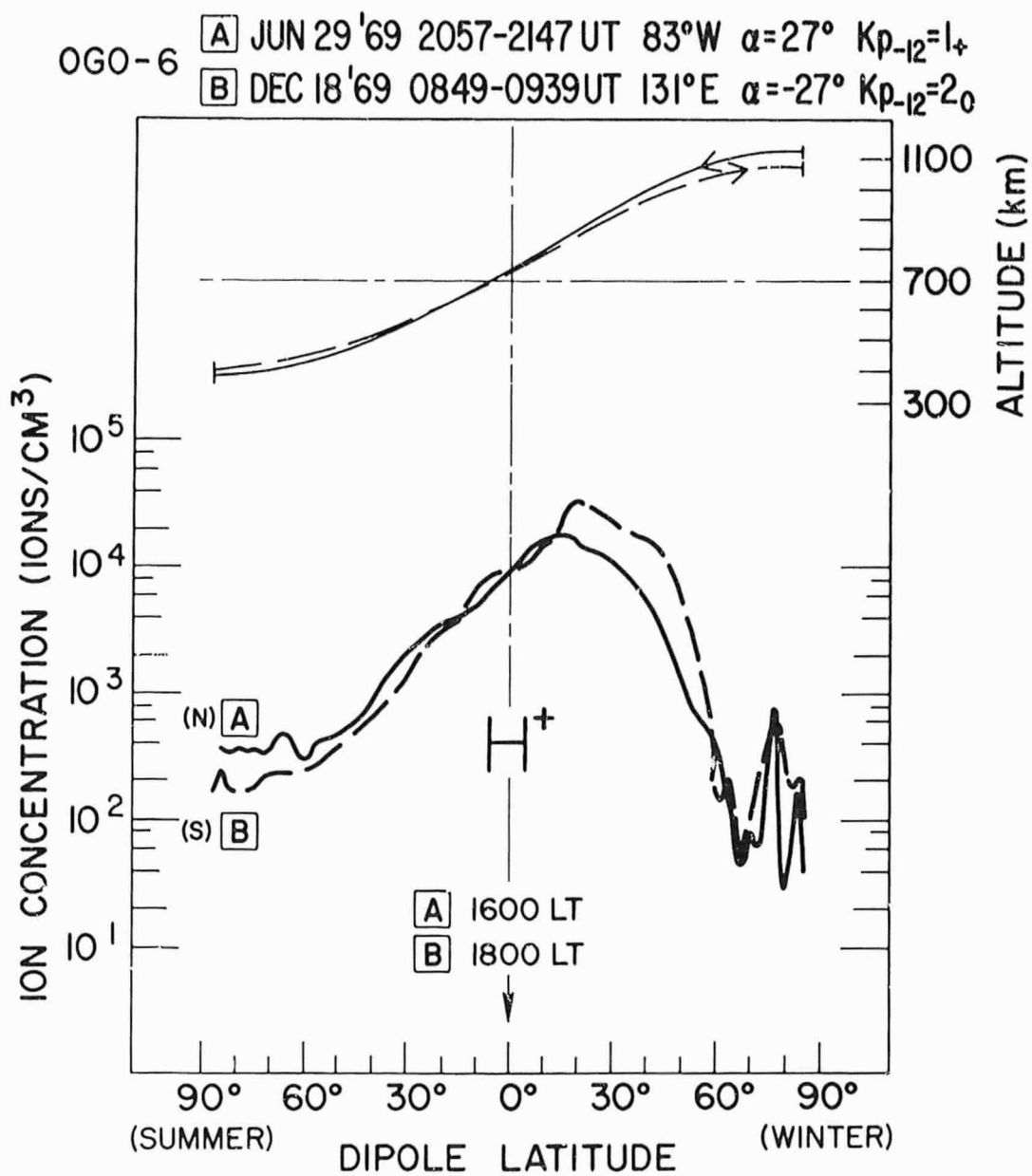


Figure 3

OGO-6 [A] JUN 29 '69 2057-2147 UT 83°W $\alpha=27^\circ$ $Kp_{-12}=1+$
 [B] DEC 18 '69 0849-0939 UT 131°E $\alpha=-27^\circ$ $Kp_{-12}=2_0$

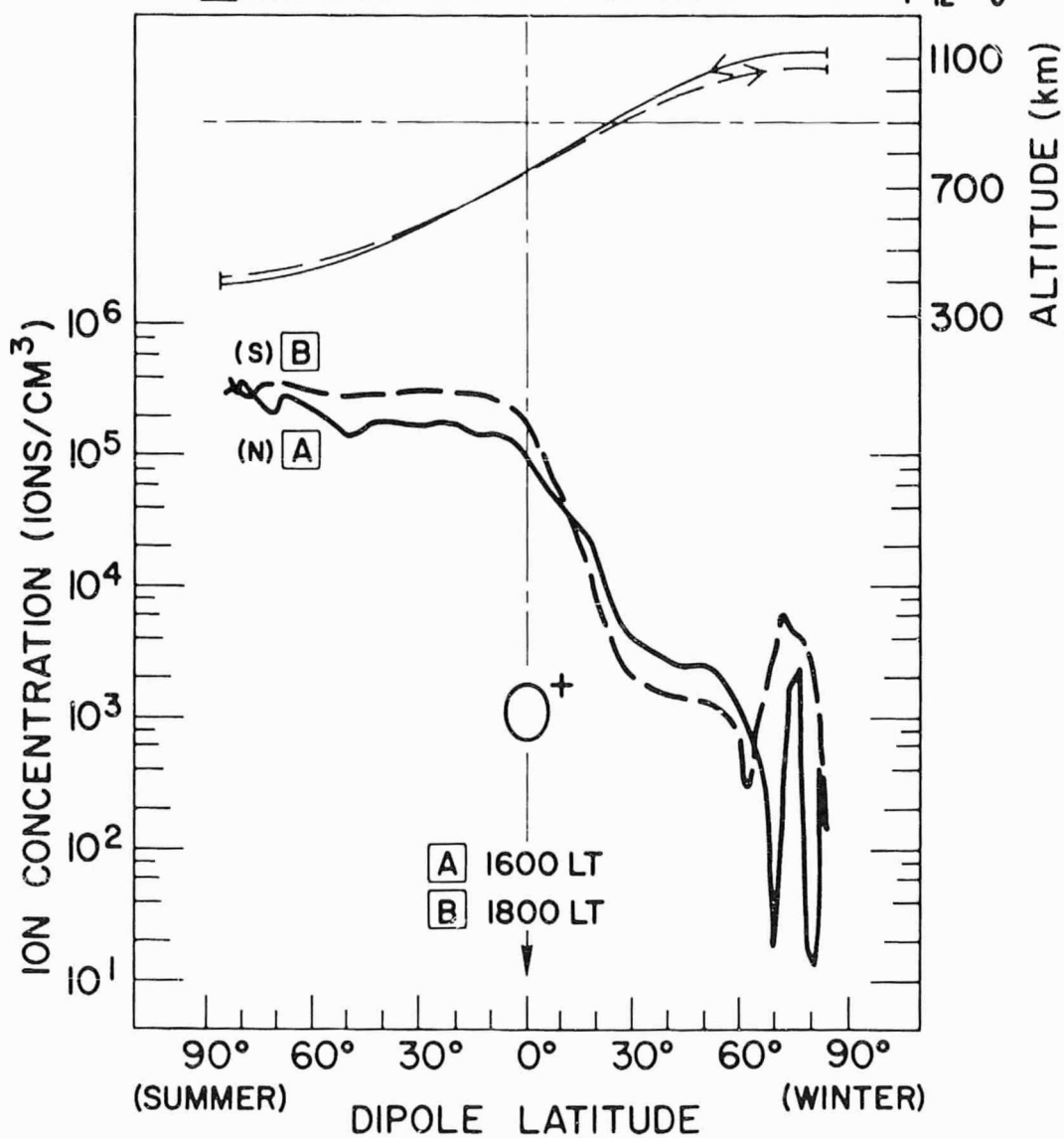


Figure 4

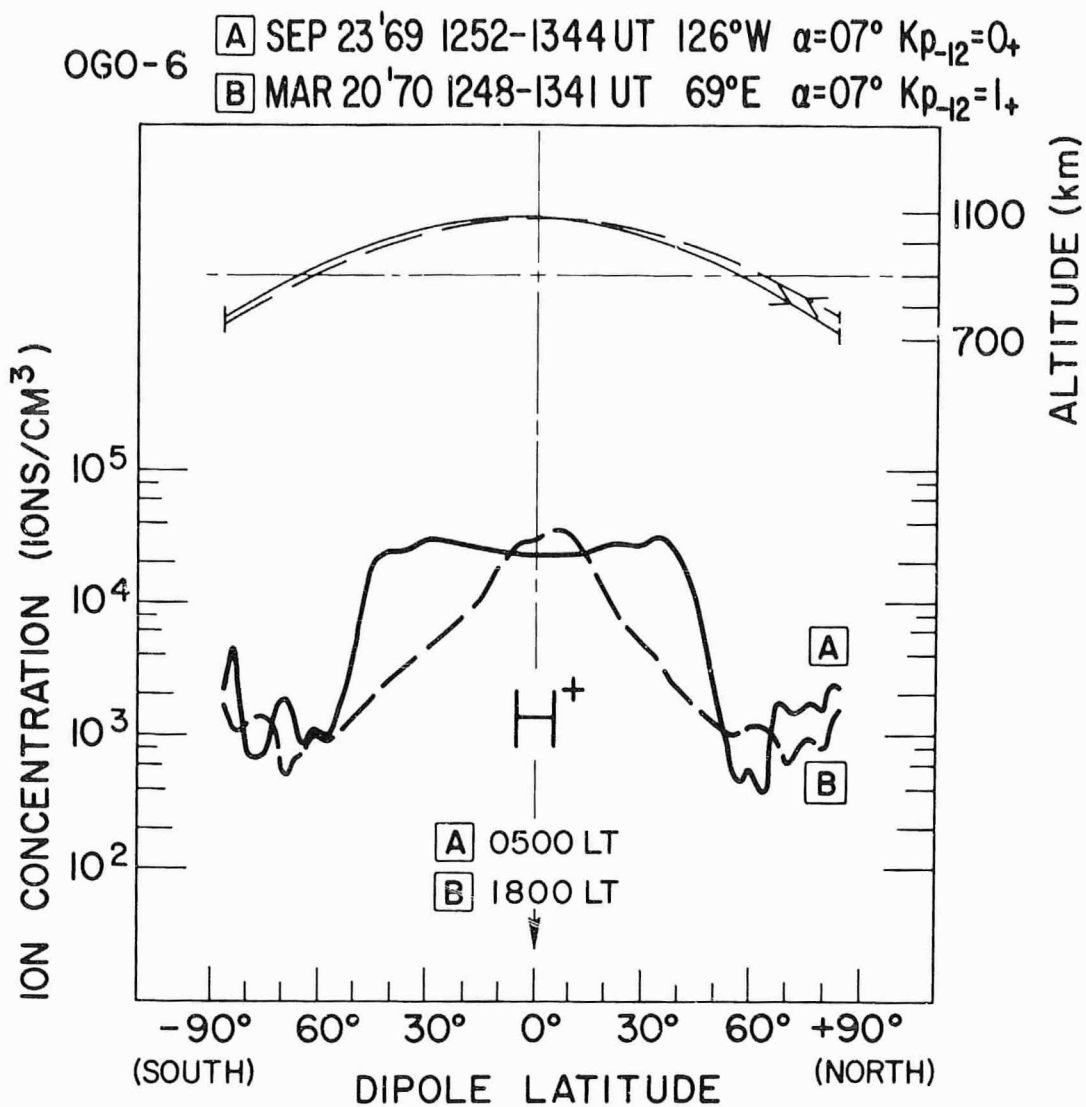


Figure 5

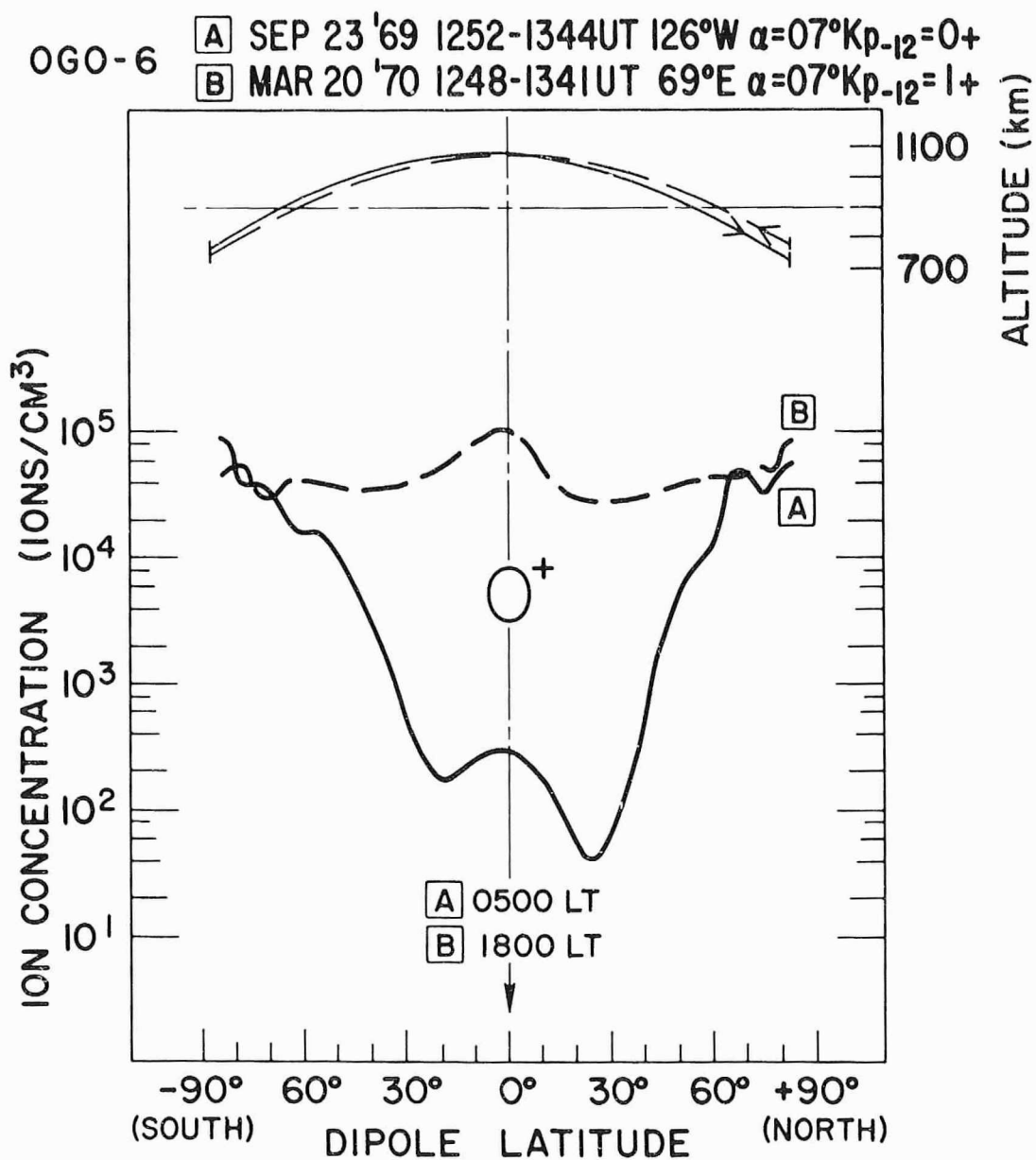


Figure 6

OGO-6 A JUL 24 '69 0413-0459 UT 125°E $\alpha=08^\circ$ $Kp_{-12}=3-$
B JUL 7 '70 0333-0419 UT 179°E $\alpha=11^\circ$ $Kp_{-12}=1_0$

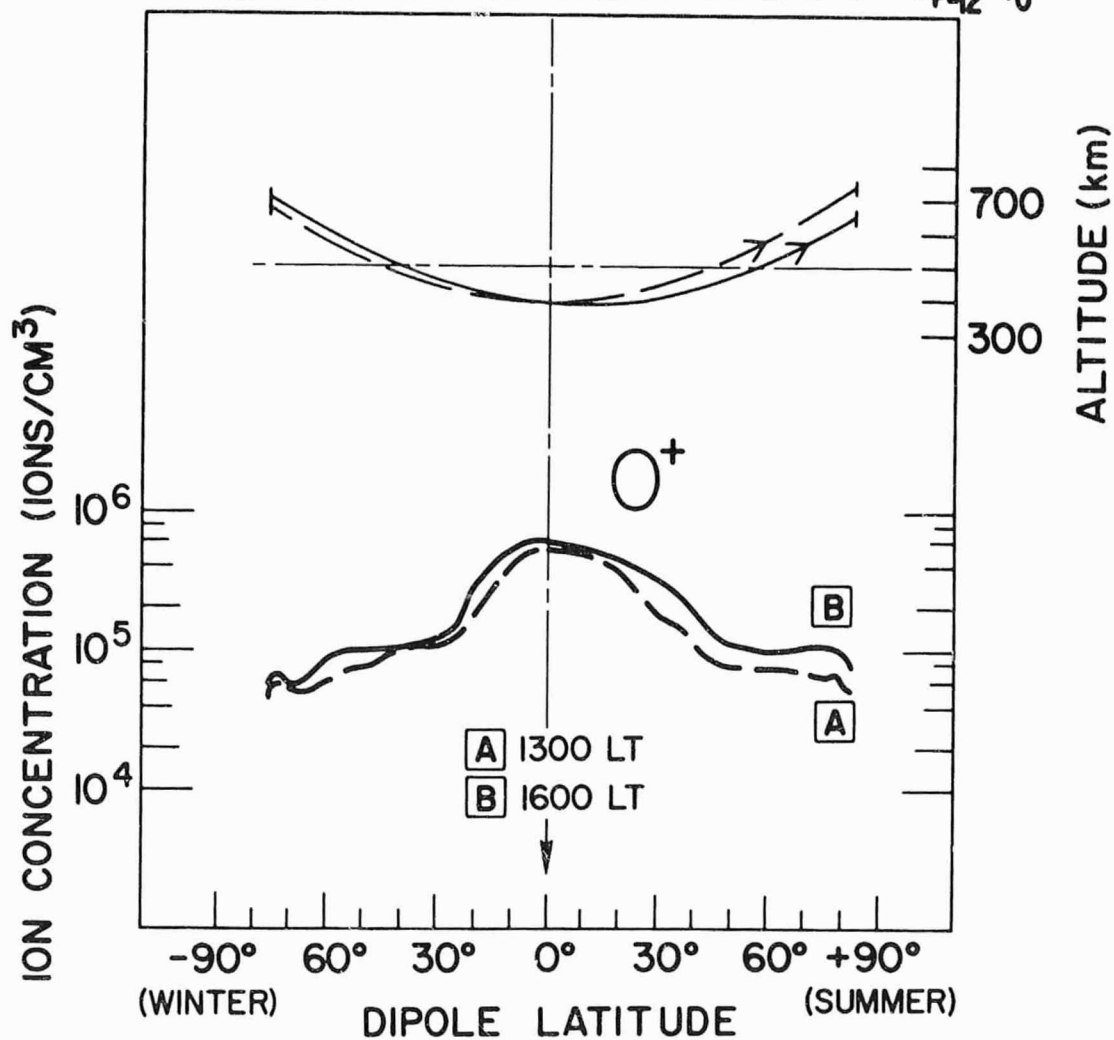


Figure 7

OGO-6 [A] JUL 25 '69 0914-1004UT 133°W $\alpha=17^\circ$ Kp-12=2-
 [B] JUL 8 '70 0826-0918UT 76°W $\alpha=17^\circ$ Kp-12=3-

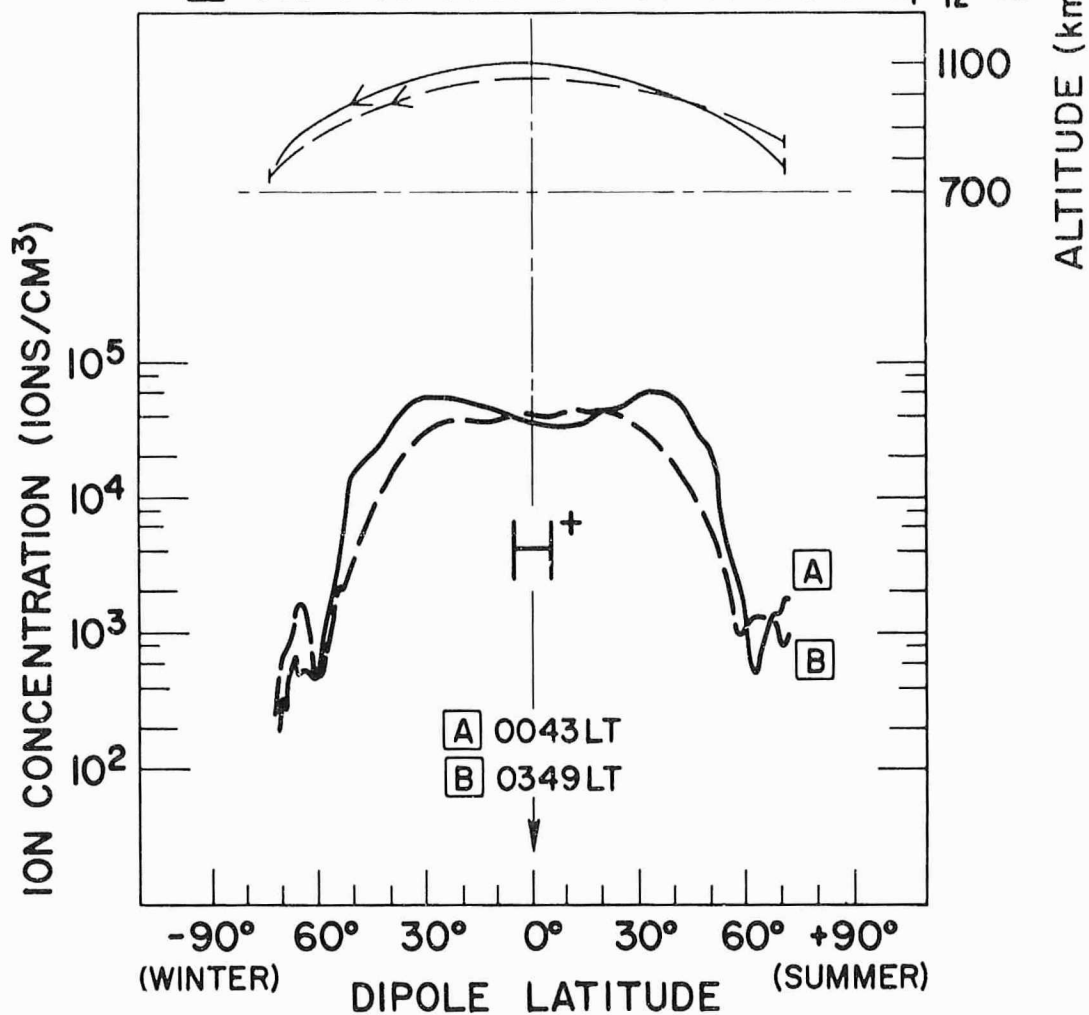


Figure 8

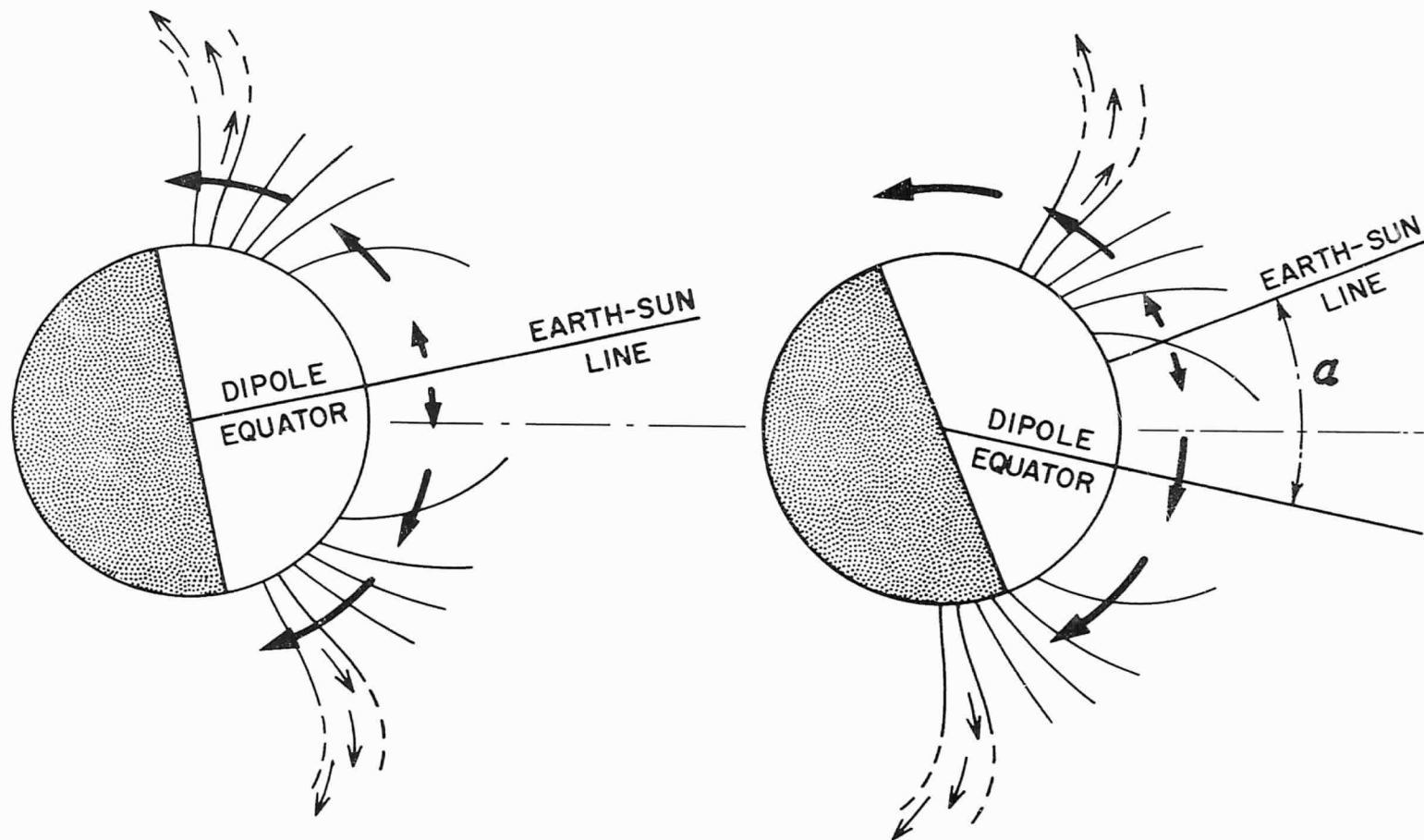
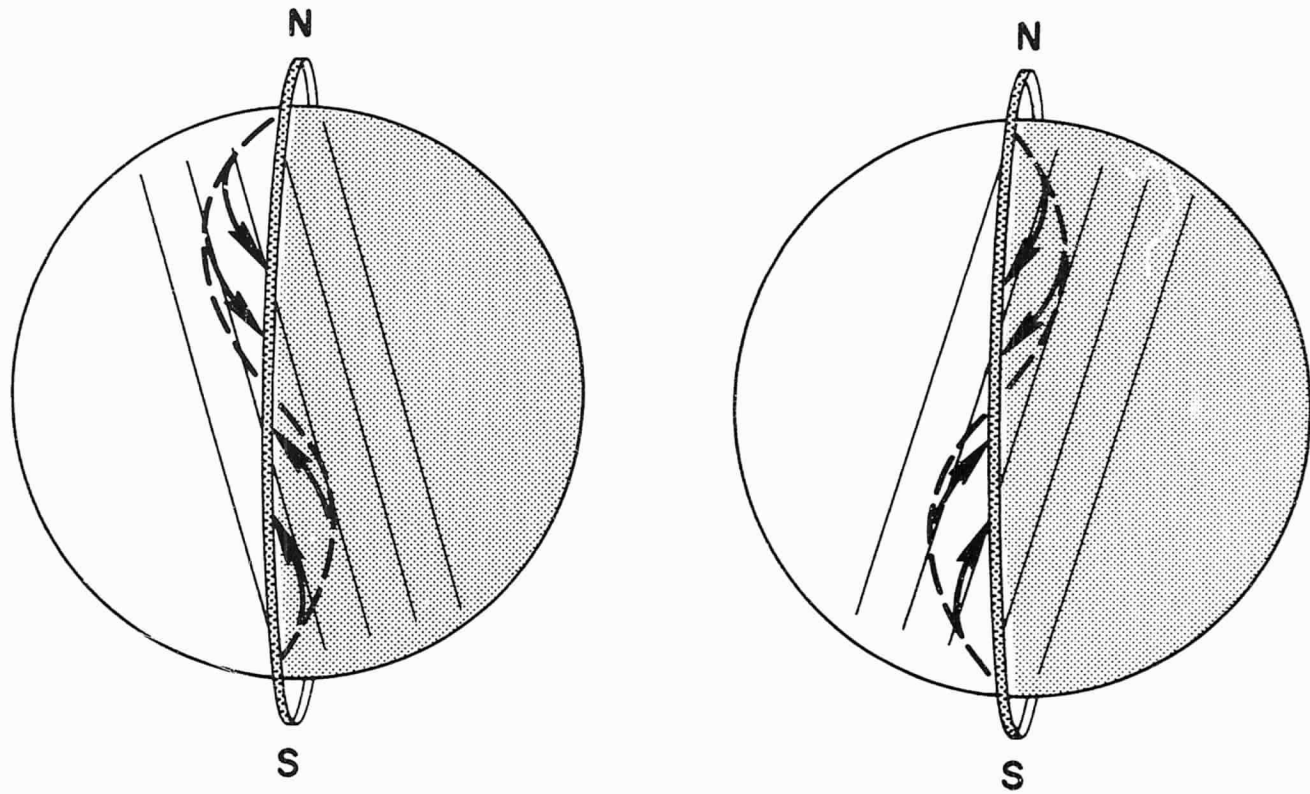


Figure 9



EFFECTIVE LOCAL TIME

Figure 10